Light-Gated Nano-Porous Capsules from Stereoisomer-Directed Self-Assemblies

Hui Chen, Yujiao Fan, Xia Yu, Vincent Semetey, Sylvain Trépout, Min-Hui Li

Light-Gated Nano-Porous Capsules from Stereoisomer-Directed Self-Assemblies

Hui Chen,[a,b] *Yujiao Fan,*[b] *Xia Yu,*[a] *Vincent Semetey,*[b] *Sylvain Trépout,*[c] *and Min-Hui Li*[b,*]

[a] Beijing Advanced Innovation Center for Soft Matter Science and Engineering, Beijing University of Chemical Technology, 15 North Third Ring Road, Chaoyang District, 100029 Beijing, P. R. China.

[b] Chimie ParisTech, PSL University Paris, CNRS, Institut de Recherche de Chimie Paris, UMR8247, 11 rue Pierre et Marie Curie, 75231 Paris Cedex 05, France.

[c] Institut Curie, Inserm US43 and CNRS UMS2016, 91405 Orsay cedex, France.

Corresponding Author: min-hui.li@chimieparistech.psl.eu

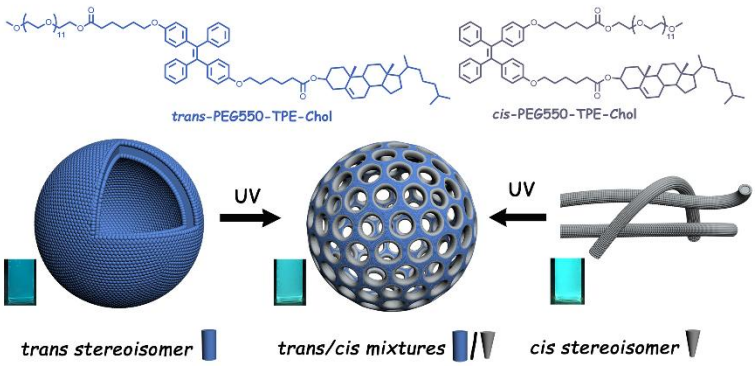

For Table of Contents use only

ABSTRACT: Structuring pores into stable membrane and controlling their opening is extremely useful for applications that require nano-pores as channels for material exchange and transportation. In this work, nano-porous vesicles with aggregation-induced emission (AIE) properties were developed from the amphiphilic polymer PEG550-TPE-Chol, in which the hydrophobic part is composed of tetraphenylethene (TPE) group and a cholesterol moiety, and the hydrophilic block is a poly(ethylene glycol) (PEG, Mn = 550 Da). Two stereoisomers, *trans*-PEG550-TPE-Chol and *cis*-PEG550-TPE-Chol, were successfully synthesized. These thermally stable stereoisomers showed distinct self-assembly behavior in water: *trans*-PEG550-TPE-Chol formed classical vesicles, while *cis*-PEG550-TPE-Chol self-assembled into cylindrical micelles. Interestingly, *trans/cis* mixtures of PEG550-TPE-Chol (*trans/cis* = 60/40), either naturally synthesized without isomers' separation during the synthesis or intentionally mixed using *trans*- and *cis*-isomers, constructed perforated vesicles with nano-pores. Moreover, under the illumination of high intensity UV light (365 nm, 15 mW/cm^2) the classical vesicles of *trans*-PEG550-TPE-Chol were perforated by its *cis* counterparts generated from the *trans*-*cis* photoisomerization, while the cylindrical micelles of *cis*-PEG550-TPE-Chol interweaved to form meshes and nano-porous membranes due to the *trans*-isomers produced by *cis*-*trans* photoisomerization. All these assemblies in water emitted bright cyan fluorescence under UV light, while their constituent molecules were not fluorescent when solubilized in organic solvent. The AIE fluorescent normal vesicles and nano-porous vesicles may find potential applications in biotechnology as light-gated delivery vehicles and capsules with nano-channels for material exchange.

KEYWORDS: amphiphilic stereoisomers, self-assembly, *trans*-*cis* photoisomerization, polymersomes, aggregation-induced emission

Capsules with regularly spaced holes in the walls exist in Nature. For example, many virus capsids have such a structure, where protein units form a rigid frame with holes.[1] In the biomimetic systems like ISCOM (immune-stimulating complexes) vaccines, cage-like structures exhibit also regular holes, but they are formed from small amphiphilic molecules including saponins, phospholipids and cholesterol.[2] Perforated vesicles (also called stomatosomes) made from small amphiphilic molecules were then clearly identified in two-amphiphiles mixtures,[3-6] such as in cetyltrimethylammonium chloride/egg phosphatidylcholines (C16TAC/EPC) in NaCl aqueous solution. All these two-amphiphiles systems have a common feature: the amphiphile 1 tends to form micelles, whereas the amphiphile 2 favors vesicle formation. The perforated vesicles are evidenced as intermediate structures in the transition from bilayer vesicles to cylindrical micelles with the increase of the ratio of amphiphile 1 over amphiphile 2.[4] Later, supramolecular capsules with nanopores were reported in dumbbell-shaped amphiphiles containing rod-core,[7] and in dendritic amphiphiles containing fluorinated-core.[8] In contrast to the multicomponent systems of small amphiphilic molecules, only one amphiphilic dendrimer is necessary to form porous membrane in these systems. The mechanism of their pore formation is more complicated and seems to be closely related to the membrane rigidity.[7, 8] It was possible to change the pore size or pore opening/closing in supramolecular capsules by external stimuli like temperature variation.[7] Structuring pores into stable membrane of capsules and controlling their opening are extremely useful for applications that require nano-pores as channels for material exchange and transportation, such as organ-on-chip tissue engineering.[9, 10] However, the number of experimental and theoretical researches in perforated vesicles is still limited.

Here we report on the perforated vesicles with nanopores formed from a mixture of *trans*- and *cis*-stereoisomers of an amphiphilic polymer PEG550-TPE-Chol (M_n = 1510 Da) with

tetraphenylethene (TPE) as the stereocenter. The hydrophilic part of the polymer is poly(ethylene glycol) (PEG550, M_n = 550 Da), and the hydrophobic part is composed of two rigid cores, the TPE and the cholesterol (Chol) moiety, and two aliphatic spacers serving as PEG-TPE and TPE-Chol connections (see Figure 1A and B). From the point of view of materials, capsules with higher molecular weight and rigid cores are more stable and robust than those made from small molecular amphiphiles. The cholesterol moiety is introduced because it is a biocompatible and bio-sourced lipophilic molecule very popular for the core-construction of self-assemblies.[11, 12] The role of TPE is three-fold. Firstly, TPE core is a stilbene-type moiety which has structurally distinct and stable *trans* and *cis* stereoisomers (Figure 1A).[13, 14] These TPE-based isomers exhibit different properties and have been reported as chemical probes for ions and biospecimens.[13] However, the influence of *trans* and *cis* configuration of TPE molecules on their self-assembly behavior was seldomly investigated.[14, 15] Thanks to the shape difference between the *trans* and *cis* isomers, their packing parameter is different and stereoisomer-directed self-assembly has been realized: normal vesicles for *trans*-PEG550-TPE-Chol (Figure 1C), cylindrical micelles for *cis*-PEG550-TPE-Chol (Figure 1D), and perforated vesicles for *trans/cis* mixture (Figure 1B). Secondly, the stilbene-type TPE can undergo *trans-cis* photo-activated isomerization under UV illumination.[16] The photo-isomerization can make the self-assembly photo-responsive. Under UV illumination of high intensity (15 mW/cm^2), both normal vesicles and cylindrical micelles tend to transform into porous vesicles, and the design of smart nanostructures is possible. Finally, TPE is a typical aggregation-induced emission (AIE) fluorophore and highly emissive in aggregate states.[17, 18] The self-assembled nanomaterials containing TPE exhibit tuneable brightness, high sensitivity and photostability.[19-21] All PEG550-TPE-Chol self-assemblies in this work are highly fluorescent under normal intensity of UV for observation and imaging (typically

< 0.5 mW/cm^2). In brief, the porous polymersomes reported here can provide a deeper insight in this intriguingly perforated membrane structure. This stilbene-type photo-sensitive system enrich the examples of photo-responsive vesicles and polymersomes, mostly based on azobenzene.[22-26] The AIE fluorescence polymersomes and cylindrical polymer micelles may also be advantageous fluorescent systems to be explored in the future as bio-imaging tools.[27]

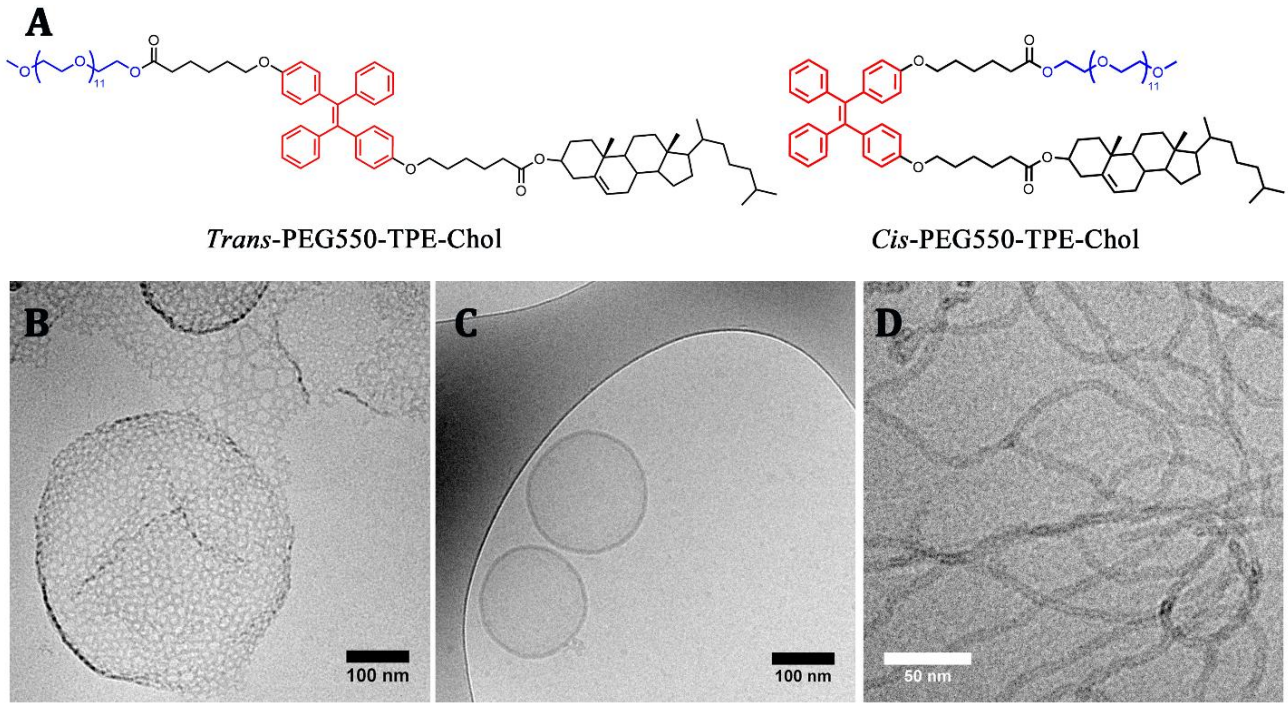

Figure 1. (A) Chemical structures of the two stereoisomers *trans*-PEG550-TPE-Chol and *cis*-PEG550-TPE-Chol. (B) Cryo-EM image of porous vesicles formed by PEG550-TPE-Chol synthesized with inherent ratio of *trans/cis* = 60/40 without isomers separation (simply noted as PEG550-TPE-Chol in the text). (C) Cryo-EM image of classical vesicles formed by *trans*-PEG550-TPE-Chol. (D) Cryo-EM image of cylindrical micelles formed by *cis*-PEG550-TPE-Chol. The method of thin-film hydration was used to perform the self-assembly.

RESULTS AND DISCUSSION

Synthesis and Characterization of PEG550-TPE-Chol and Their Stereoisomers

The synthesis of amphiphilic molecules PEG550-TPE-Chol was performed through the synthetic route as shown in Supplementary Scheme S1. Initially, Ti-catalyzed McMurry coupling reaction was employed to provide TPE-2OMe *trans/cis* mixture (Figure S1). Because *trans*- and *cis*- isomers of TPE-2OMe have nearly identical retardation factor (R_f) on thin-layer chromatography (TLC), they cannot be separated easily by column chromatography. If no separation between *trans*- and *cis*-isomers was made during the whole synthetic procedure, the final product PEG550-TPE-Chol contained nearly the equivalent rate of *trans*- and *cis*-isomers (see Figure S3 for ^{1}H NMR spectrum, calculated ratio *trans*/*cis* = 60/40, calculation detail will be discussed below).

The *trans*- and *cis*-PEG550-TPE-Chol were then prepared with the separated intermediate derivatives *trans*-TPE-2COOMe and *cis*-TPE-2COOMe, respectively (Figure 2A and Scheme S2), where two big and polar substituents methyl 6-hexanoate replaced the methyl groups in TPE-2OMe. Indeed, the two isomers of TPE-2COOMe showed different R_f, 0.52 and 0.44, respectively, on TLC using petroleum ether and ethyl acetate (10:1 volume ratio) as eluent solvents (Figure S10). They were successfully separated by careful column chromatography. The single crystal of the pure isomer with R_f = 0.52 was acquired by slow evaporation of solvents. Its crystal structure was characterized by X-rays diffraction (see Figure S11 and Table S1). The results clearly show that the functionalized phenyl groups are located on the opposite sides of the central double bond. Unambiguously, the isomer collected firstly in column chromatographic experiment with R_f =0.52 corresponded to the *trans*-TPE-2COOMe. The isomer collected later with R_f =0.44 was *cis*-TPE-2COOMe. Both isomers are very stable and can be stored at room temperature. ^{1}H NMR spectra (Figure 2A) show clearly the difference of chemical shifts between

H_a (H_b) for *trans*-isomer and H_a' (H_b') for *cis*-isomer at δ around 6.6 ppm (6.9 ppm). The *trans*- and *cis*-TPE-2COOMe were then used as starting materials to synthesize corresponding amphiphilic stereoisomers, respectively (see SI and Scheme S2), *via* hydrolysis reaction to get *trans* and *cis*-TPE-2COOH followed by a first esterification reaction with cholesterol and a second esterification with methoxy-poly(ethylene glycol) (mPEG550-OH). The structures of all the compounds were confirmed by ^{1}H NMR, ^{13}C NMR and high-resolution mass spectrometry (HRMS) (Figure S4-S9, Figure S12). *Trans*- and *cis*- isomers were stable and maintained their geometry along the synthetic process from TPE-2COOMe to PEG550-TPE-Chol (see Figure S13 and S14). For the final amphiphilic stereoisomer *trans*-PEG550-TPE-Chol, the ^{1}H NMR analysis detected tiny *cis*-signals of Ha' next to the main *trans*-signals of H_a (Figure S15 and Figure 2B). Careful peak integration revealed that the *trans*-PEG550-TPE-Chol contained around 5% of *cis* isomer. The same result was also observed for the *cis*-PEG550-TPE-Chol (Figure S15 and Figure 2C), which contained about 5% of *trans* isomer. This small imperfection can be explained as follows. In order to obtain enough final compounds of *trans*- and *cis*-PEG550-TPE-Chol, TPE-2COOMe have been synthesized in great quantity. The large-scale separation of *trans*- and *cis*-TPE-2COOMe by manual column chromatography are not perfect because their R_f values are too close (see Figure S10) and it is difficult to separate them completely. Nevertheless, we will show hereinafter this trace impurity will not influence the self-assembly behaviors of both *trans*- and *cis*- PEG550-TPE-Chol.

The molecular weight of *trans*- and *cis*- PEG550-TPE-Chol were then analyzed by size exclusion chromatography (SEC) (Figure S16). Their SEC peaks are well separated, and the elution time of *trans*-isomer is longer than that of its *cis* counterpart. This observation is completely coherent with the fact that the shapes of *trans*- and *cis*- PEG550-TPE-Chol are quite

different, even though their molecular weight are the same (M_n = 1510 Da). Because of the presence of TPE moieties, both *trans*- and *cis*-PEG550-TPE-Chol exhibit aggregation-induced emission under UV light around 365 nm. As shown in Figure S17, they are not fluorescent when they are solubilized in solution of acetone, but highly fluorescent in aggregated states formed from acetone/water mixture.

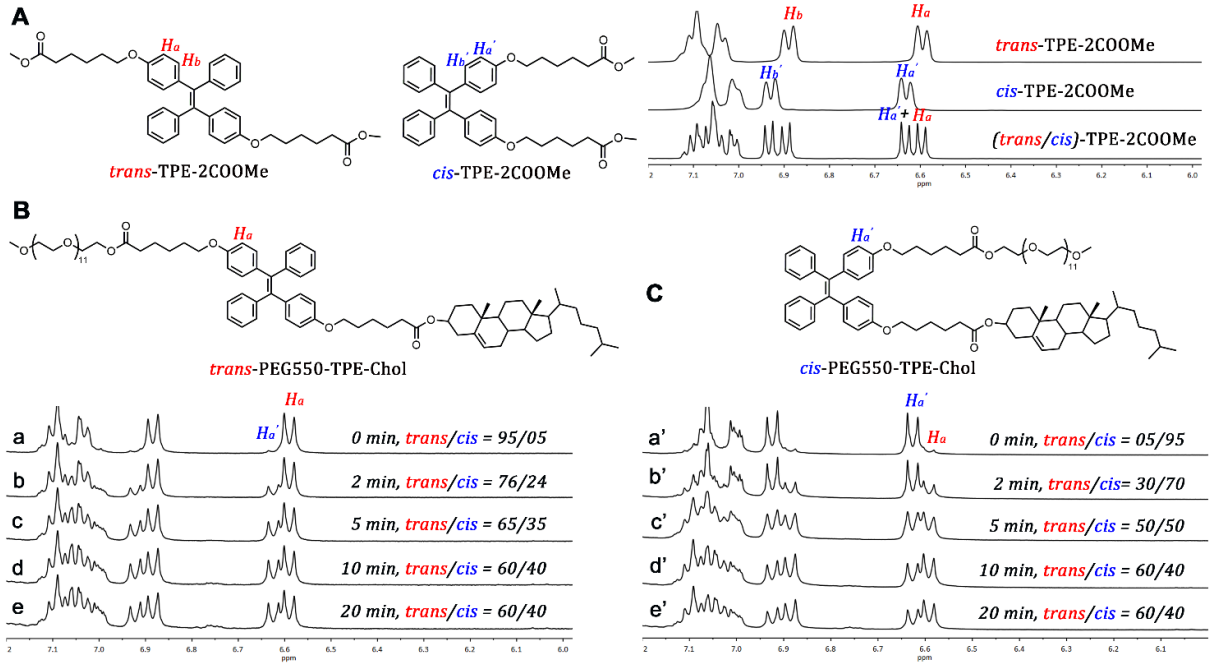

Figure 2. (A) Chemical structure of *trans*-TPE-2COOMe and *cis*-TPE-2COOMe and the partial ^{1}H NMR spectra of the *trans*-TPE-2COOMe, *cis*-TPE-2COOMe and (*trans*/*cis*)-TPE-2COOMe mixture (400 MHz, $CDCl_3$). (B) Chemical structure of *trans*-PEG550-TPE-Chol, and partial ^{1}H NMR spectra of *trans*-PEG550-TPE-Chol in $CDCl_3$ after UV irradiation (365 nm, 15 mW/cm^2) with different duration: (a) t = 0 min, (b) t = 2 min, (c) t = 5 min, (d) t = 10 min, (e) t = 20 min. (C) Chemical structure of *cis*-PEG550-TPE-Chol, and partial ^{1}H NMR spectra of *cis*-PEG550-TPE-Chol in $CDCl_3$ after UV irradiation (365 nm, 15 mW/cm^2) with different duration: (a') t = 0 min, (b') t = 2 min, (c') t = 5 min, (d') t = 10 min, (e') t = 20 min. The abscises of all NMR spectra are scaled from 6.0 to 7.2 ppm for clarity.

The possibility to activate the isomerization between two stereoisomers by heating and by UV illumination has been checked. Both isomers are rather thermally stable as shown by ^{1}H NMR spectra in Figure S18 and Figure S19. Heating their solution in DMSO up to 70℃ for 30 min cannot induce *trans*-to-*cis* or *cis*-to-*trans* isomerization. When heating at 120℃ for 24h, only 12-14% of isomerization occurs. Under weak UV light (365 nm, < 0.5 mW/cm^2), both isomers in solution are also stable during normal observation time (in the order of minutes), as shown by ^{1}H NMR spectra in Figure S20. Typically, the intensity of UV light (365 nm) for thin-layer-chromatography (TLC) detection during the synthesis is ≤ 0.5 mW/cm^2, and that in spectrofluorometer is 0.25 mW/cm^2. After 2 min of illumination by UV light (365 nm) of 0.5 mW/cm^2, no photoisomerization can be detected (Figure S20). In contrast, photo-isomerization of isomers in solution takes place readily when increasing the UV intensity to 15 mW/cm^2 as shown by ^{1}H NMR spectra in Figure 2B and 2C. *Trans* and *cis*-PEG550-TPE-Chol exposed to UV light (365 nm) of 15 mW/cm^2 for 2 min undergo already 19% and 25% of isomerization, respectively. After 10 min of illumination, both *trans*-to-*cis* and *cis*-to-*trans* isomerization reach a stationary state with *trans/cis* ratio of 60/40. The *trans*-isomer is in a little excess compared to *cis*-isomer, because the *trans*-PEG550-TPE-Chol is more photo-stable than its *cis* counterpart and the *cis*-isomer has a faster isomerization rate than that of *trans*-isomer. No significant photo-cyclization was observed for both *cis* and *trans*-PEG550-TPE-Chol after 10 min of illumination (nearly no ^{1}H NMR signals at 6.7 -6.8 ppm).[16, 28]

Self-Assembly of *Trans*- and *Cis*-PEG550-TPE-Chol and Their Mixtures: Vesicles, Perforated Vesicles and Cylindrical Micelles

Considering the molecular weight (M_n = 1510 Da) of PEG550-TPE-Chol, which is higher than traditional small amphiphilic molecules like lipids EPC, we prepared the vesicles using thin-film

hydration method at high temperature (T = 65 °C) to accelerate the sample hydration and polymer self-organization. Typically, the chloroform solution of PEG550-TPE-Chol or their stereoisomer (0.5 *wt*%) was uniformly deposited on the surface of a roughened Teflon plate, followed by drying in vacuum to remove all solvent and to get a thin polymer film. Then the thin film sample was hydrated with deionized water at 65 °C for 48 h in a sealed bottle. In order to check if there were any *trans*-*cis* isomerization of amphiphiles during the self-assembling process, the obtained self-assemblies of *trans*- and *cis*-PEG550-TPE-Chol were recovered, respectively, by freeze-drying, and then dissolved in deuterated DMSO and analyzed by ^{1}H NMR. As shown in Figure S21, the *trans/cis* ratios of both *trans*- and *cis*-PEG550-TPE-Chol do not show any change and keep being 95/5 and 5/95, respectively, after the self-assembling process, which prove the absence of the isomerization.

The morphologies and sizes of the self-assemblies were characterized by cryo-electron microscopy (cryo-EM) and dynamic light scattering (DLS). PEG550-TPE-Chol (*trans*/*cis* = 60/40) self-assembled into perforated vesicles, while *trans*-PEG550-TPE-Chol self-assembled into normal vesicles and *cis*-PEG550-TPE-Chol into cylindrical micelles (Figure 1B, C and D, Figure S22-24). The statistical sizes distributions of vesicles measured by DLS are shown in Figure S25, which indicate multimodal size distributions including nanovesicles and giant vesicles. Indeed, different sizes of vesicles were observed as shown in Figure S23, which was normal with film hydration technique. The length of cylindrical micelles reaches several hundreds of nanometers until several micrometers, and some interconnected points (Y-junctions) are also visible (Figure 1D and Figure S24). The formation of Y-junctions in the cylindrical micelles have already reported in diblock copolymers poly(*1,2*-butadiene-*b*ethylene oxide) (PB-PEO) in water.[29] Note that the trace amount of *cis*-isomer (5%) in the *trans*-PEG550-TPE-Chol

did not influence the formation of vesicles which represent the absolute majority of the morphologies. Meanwhile, *cis*-PEG550-TPE-Chol formed only cylindrical micelles with a few of Y-junctions despite the presence of 5% *trans*-isomer according to the collected cryo-EM images. The membrane thickness of vesicles and the diameter of cylindrical micelles were evaluated from the FWHM (Full Width at Half Maximum) of the electronic density profile perpendicular to the membrane through statistical analysis of about 30 different vesicles in the cryo-EM images. The thickness of vesicle membrane for *trans*-PEG550-TPE-Chol was measured as 7.5 ± 0.5 nm, the diameter of cylindrical micelles for *cis*-PEG550-TPE-Chol as 6.5 ± 0.5 nm and the thickness of the membrane of perforated vesicles for PEG550-TPE-Chol as 7.3 ± 0.5 nm.

When the stereo-structure changes from *trans*- to *cis*-type, the morphological transition of self-assemblies from vesicles to cylindrical micelles should be driven by the minimization of the interfacial energy. Following qualitatively the theory of Israelachvili *et al.*,[30, 31] the packing parameter $p = v/al$ of *trans*-PEG550-TPE-Chol in aqueous solution should be around 1 for vesicle formation, while the p value of *cis*-PEG550-TPE-Chol should be smaller and approach 1/2 for cylindrical micelle formation (where v is the hydrophobic volume, a the optimal interfacial area, and l the length of the hydrophobic block normal to the interface). Here, the chemical structures are the same for both isomers, so their steric shapes dictate their packing parameter in the self-assemblies. Photo-switchable transition between vesicles and cylindrical micelles caused by *trans-cis* isomerization of azobenzene has also been reported.[32] A schematic representation of the self-assemblies of *trans*- and *cis*-PEG550-TPE-Chol and their molecular packing is given in Figure 3A and 3B. The plausible molecular models of the hydrophobic part for *trans*- and *cis*-PEG-TPE-Chol in the bilayer membranes and cylindrical micelles are

illustrated in Figure S26, with the lengths of l_{trans} = 4.54 nm and l_{cis} = 4.05 nm. The thickness of vesicle membrane (e = 7.5 nm) is between l_{trans} (4.54 nm) and $2l_{trans}$ (9.08 nm), the diameter of cylindrical micelles (d_c = 6.5 nm) is also between l_{cis} (4.05) and $2l_{cis}$ (8.10 nm). Therefore, both *trans*- and *cis*-PEG-TPE-Chol in the bilayer membrane and in the cylindrical micelles should be packed in the interdigitated way as shown in Figure 3A and 3B. Cholesterol is a versatile building block which supports the formation of bilayer membranes,[33] and fibril structures[34, 35] due to its molecular rigidity, self-assembling nature, asymmetric carbons, *etc*. For the cylindrical micelles formed by *cis*-PEG-TPE-Chol, along the cylindrical axis the cholesterol moieties turn around this axis to form the cylindrical micelles, whose cross-section is round as shown in Figure S24.

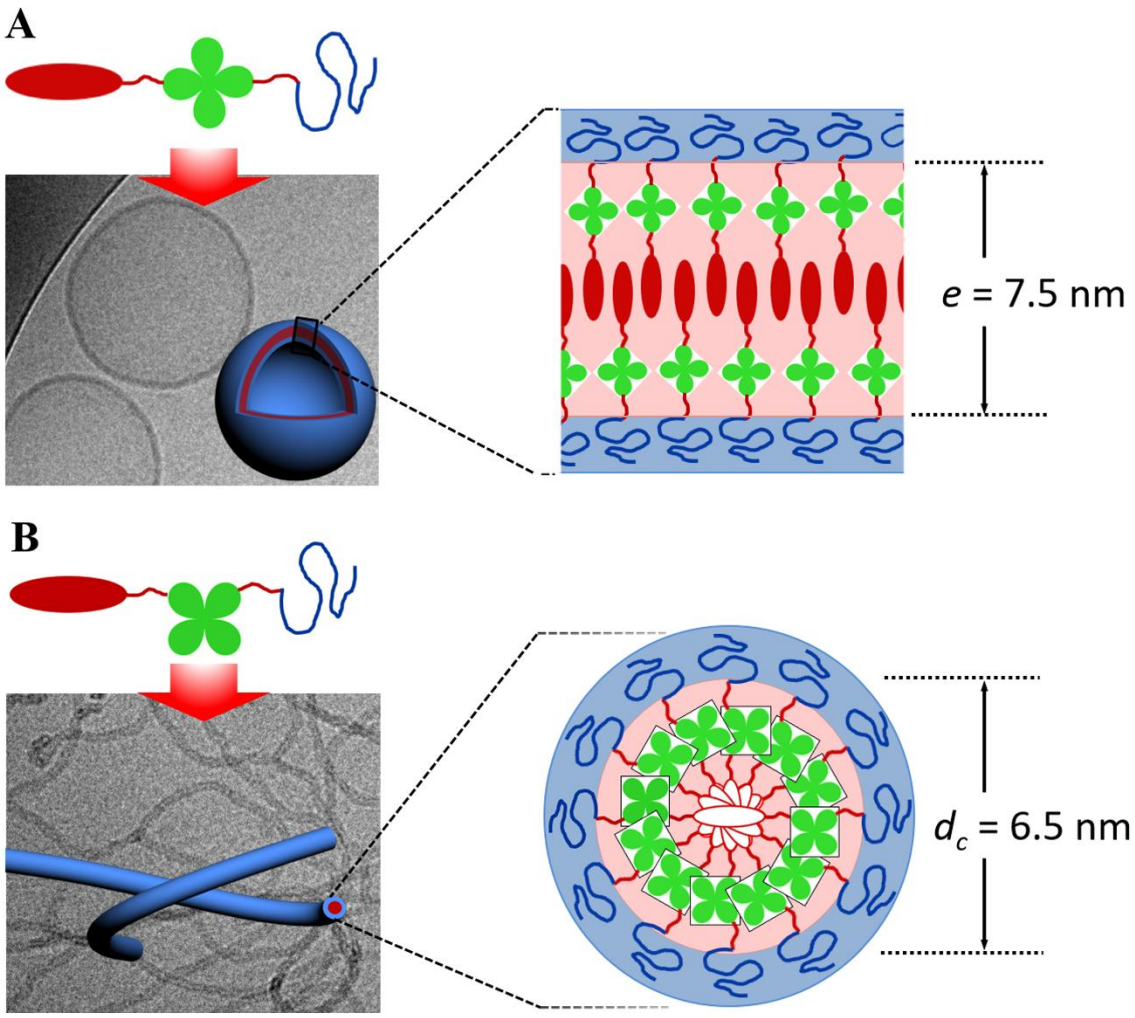

Figure 3. The morphologies models of polymersomes (A) and cylindrical micelles (B) formed by *trans*-isomer and *cis* isomer, respectively. The red ellipsoid represents the cholesterol moiety, and the green trefoil the TPE group. The red line represents the aliphatic spacer, and the blue line the PEG550 chain. In the cylindrical micelle model, empty red ellipsoids are used to represent the cholesterol moiety in order to highlight molecular organization along the cylinder long axis.

Interestingly the PEG550-TPE-Chol forms perforated membranes and vesicles (see Figure 1B and Figure S22), similarly to the mixture of small molecular amphiphiles, *e.g.,* C16TAC and EPC.[3] The innovation here is the PEG550-TPE-Chol is a stereoisomers-mixture synthesized as

one compound, simply and inherently without the tedious separation of intermediates *trans*- and *cis*-isomers during the synthetic procedure. Further, we prepared artificially the mixtures of both stereoisomers to get *trans*/*cis* ratio of 60/40, the same as inherently synthesized PEG550-TPE-Chol, and then performed the self-assembling by film hydration in the identical conditions. Figure 4 shows the representative morphologies of its self-assemblies observed by cryo-EM, which are the same as those obtained with inherently synthesized PEG550-TPE-Chol (Figure 1B).

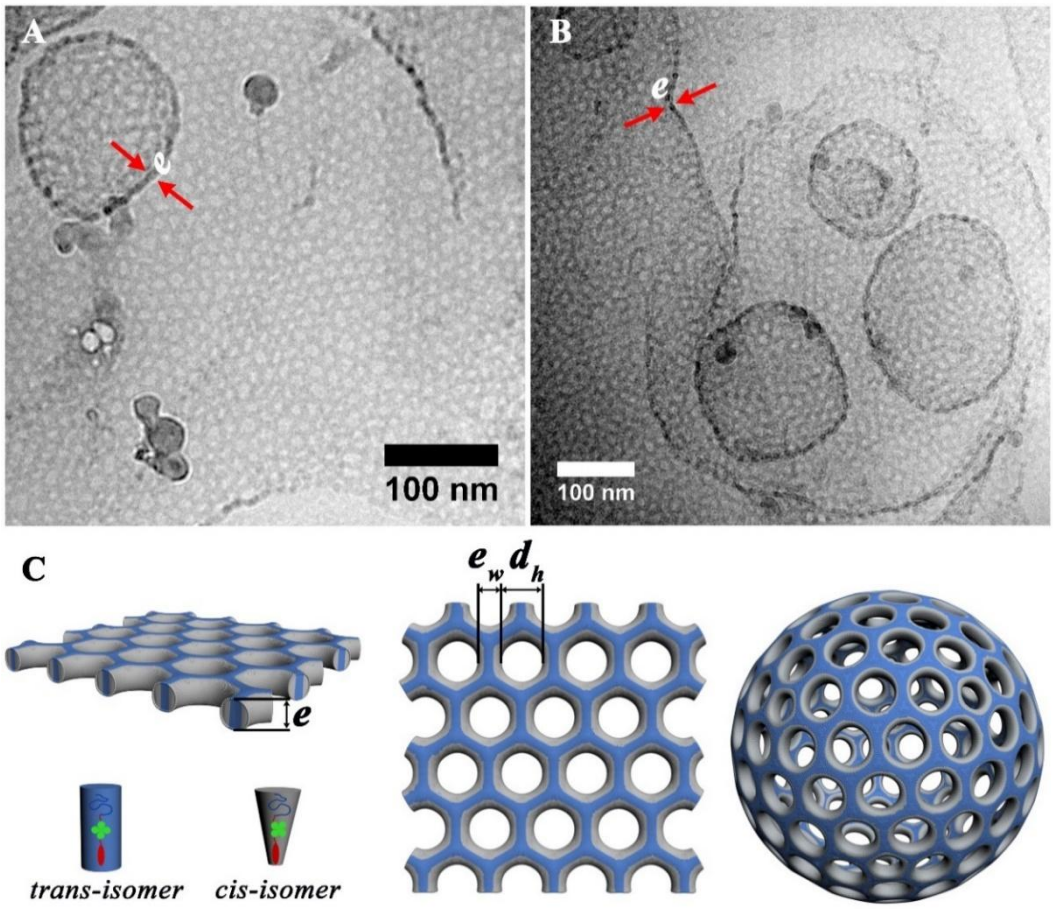

Figure 4. (A, B) Cryo-EM images of self-assemblies obtained from *trans*- and *cis*-PEG550-TPE-Chol mixtures intentionally prepared at the ratio *trans/cis* = 60/40. The red arrows show the examples of vesicle edges or edges of folded membranes. (C) Schematic representation of

perforated membrane and nano-porous polymersomes. The small blue cylinder represents the *trans*-PEG550-TPE-Chol that is preferably assembled in flat areas with low curvature. The gray cone represents the *cis*-PEG550-TPE-Chol that is likely aggregated at the edges of holes with high curvature.

The scenario of porous membrane formation can be explained as follows. Micelle-forming *cis*-isomers in a bilayer membrane try to impose a positive curvature on the constituent monolayers (leaflets). The monolayers may remain united to a flat bilayer only up to a critical concentration of the micelle-forming *cis*-isomers. Above this critical point, edges may form, which would contain predominately the micelle-forming *cis*-isomers and assemble into hemicylindrical structures with a negative curvature (the holes). With *trans*/*cis* ratio of 60/40, the hole part and strand part have similar proportion in the mesh-like membrane. Table 1 summarizes the measured values for bilayer membrane thickness (e), cylindrical micelle diameters (d_c), pore diameter (d_h) and the minimal wall thickness (e_w) between two pores (see Figure 4 for the definition). We found $e_w \geq d_c$, which means the narrowest place of the wall is almost composed of the cross-section of two face-to-face hemicylinders.

Table 1. Size characterization of different morphologies of *trans-/cis* isomers and mixtures by cryo-EM.

Sample	Membrane thickness e (nm)	Cylindrical micelle diameter d_c (nm)	Pore diameter d_h (nm)	Pore wall thickness e_w (nm)
trans-PEG550-TPE-Chol (*trans/cis* = 95/5)	7.5 ± 0.5	-	-	-
Isomers mixture (*trans/cis* = 60/40)	7.3 ± 0.5	-	9.0 – 27.0	6.9 – 7.6

cis-PEG550-TPE-Chol (*trans/cis* = 5/95)	-	6.5 ± 0.5	-	-

AIE and Photo-Responsive Properties of Vesicles, Perforated Vesicles, and Cylindrical Micelles

All self-assemblies of both *trans*- and *cis*-PEG550-TPE-Chol, as well as of their mixtures are fluorescent under UV light because of TPE moieties. Once the TPE self-assembled in hydrophobic domain of nanostructures, the physical constraints and space limitations enable to restrict the intramolecular rotation of phenyl groups around the singles bonds in TPE. Under UV illumination, the non-radiation decay of excited TPE is locked and the radiative decay channel turns on, consequently nanostructures become efficiently emissive. Their UV-visible absorption spectra and fluorescence spectra are shown in Figure 5. The quantum yields are 0.12 and 0.15 for *trans*- and *cis*-PEG550-TPE-Chol assemblies, respectively.

Since both *trans*- and *cis*- isomers can undergo *trans*-to-*cis* and *cis*-to-*trans* isomerization under UV illumination, we have also studied the morphological transformation of their self-assemblies under UV light of higher intensity. Typically, the aqueous dispersions of self-assemblies of *trans*- and *cis*-PEG550-TPE-Chol were exposed to UV light (365 nm, 15 mW/cm^2) for 30 min, respectively. One part of the irradiated sample was investigated by cryo-EM, and the rest was first freeze-dried and then solubilized in $CDCl_3$ for analysis by ^{1}H NMR. ^{1}H NMR spectra (Figure S27) show that after UV illumination, the *trans/cis* ratios in both samples become 60/40, in agreement with the results obtained in solution samples exposed to UV light (Figure 2B and 2C). It is also notable that photocyclization of TPE moiety begin to occur as a trace of new peak emerged at 6.7 -6.8 ppm for both *cis* and *trans*-PEG550-TPE-Chol after 30 min illumination (Figure S27). Cryo-EM images of both UV treated samples are shown in Figure 5C

and 5D as well as in Figure S28 and S29. Vesicles of *trans*-PEG550-TPE-Chol initially with homogeneous and smooth surface were perforated by the *cis*-isomers resulted from the photoisomerization, while cylindrical micelles of *cis*-PEG550-TPE-Chol under UV interweaved to form meshes and perforated membranes because of the appearance of *trans*-isomers. The perforated membranes obtained from cylindrical micelles were less structured (Figure 5D) than those from smooth vesicles, probably for the kinetic reason, *i.e.,* because of the slow rate of the fusion between separated cylindrical micelles. As expected, perforated vesicles and membranes of PEG550-TPE-Chol did not show significant change upon UV light exposure (see cryo-EM images in Figure S30), because of simultaneous *trans*-to-*cis* and *cis*-to-*trans* isomerization.

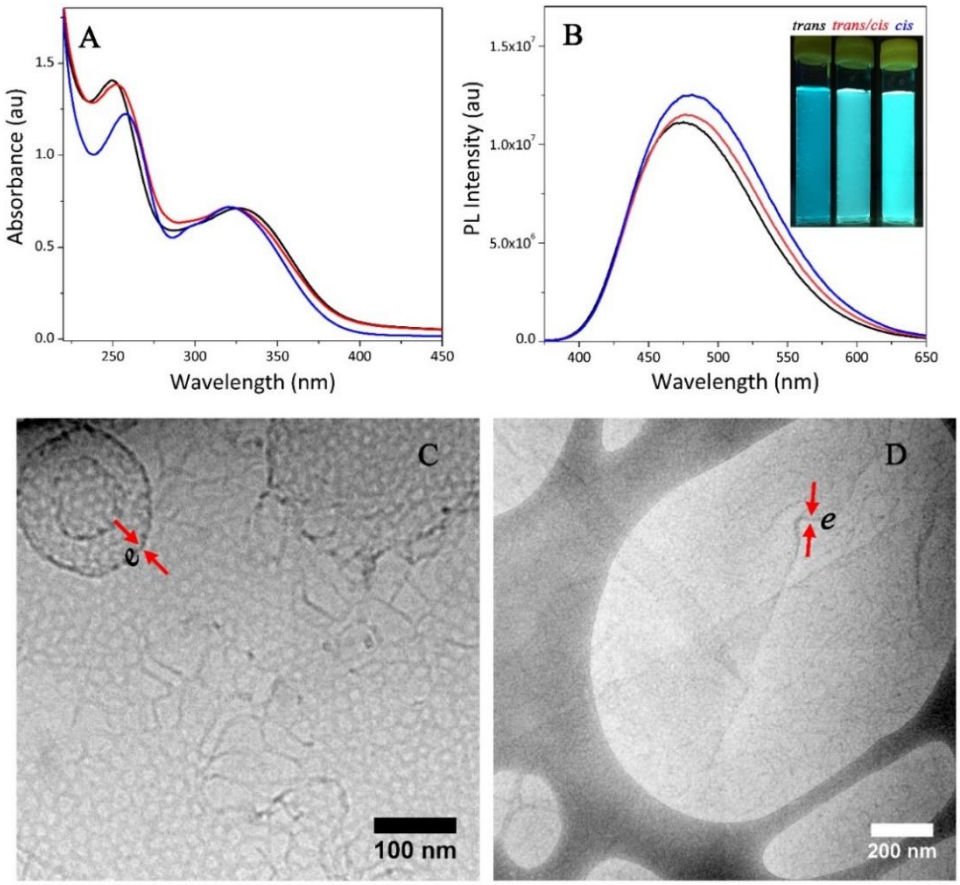

Figure 5. (A) The UV-visible absorption spectra of *trans* assemblies (black line), *cis* assemblies (blue line) and the assemblies formed by *trans/cis* mixtures (*trans/cis* = 60/40) (red line).

(Concertration: 6.7 x10^{-2} mg/ml). (B) The photoluminescence (PL) spectra of *trans* assemblies (black line), *cis* assemblies (blue line) and the assemblies formed by *trans/cis* mixtures (*trans/cis* = 60/40) (red line). (concentration: 6.7 × 10^{-2} mg/ml; excitation wavelength: 352 nm, 0.5 mW/cm^2). The inset photos are the dispersions of self-assemblies taken under 365 nm UV light (0.5 mW/cm^2). (C) and (D) Cryo-EM images of perforated membranes and vesicles obtained by irradiation of vesicles of *trans*-PEG550-TPE-Chol (C) and of cylindrical micelles of *cis*-PEG550-TPE-Chol (D) after 30 min of irradiation by UV light (365 nm, 15 mW/cm^2). The red arrows show the examples of vesicle edges or edges of folded membranes.

The transition from the "closed" to "open" states (with pores of 9-27 nm diameters) for polymersomes formed by *trans*-PEG550-TPE-Chol, triggered by UV light, indicated that this kind of polymersomes could be used to encapsulate guest molecules of big sizes and release them in a controlled way. The tetramethylrhodamine isothiocyanate–dextran (TRITC-Dextran, MW = 4400 Da) was used as a model molecule for test. The details of encapsulation and release experiments were described in SI. Figure S33 demonstrates the release percentages after 0, 15 and 30 min of UV irradiation, 50% of TRITC-Dextran being released after 30 min of irradiation.

Big morphologies like giant vesicles and large membranes also co-existed with nano-vesicles in the self-assemblies of PEG550-TPE-Chol (*trans/cis* = 60/40) synthesized without isomers' separation during the synthesis. Cryo-EM allows to detect the nanostructures in detail as shown in Figure 4 (and Figure S22-23, S28-S30), but it cannot visualize the giant structures wholly. Therefore, epifluorescence optical microscopy was also used for observation of the giant vesicles formed by PEG550-TPE-Chol (Figure 6). Under UV light, giant vesicles are cyan fluorescent as shown in Figure 6. With the increase of UV illumination time, the membrane becomes fluctuating, probably because the hole parts and strand parts interchange continuously resulting

from the simultaneous *trans-cis* and *cis-trans* isomerization in PEG550-TPE-Chol. Even with this high intensity UV of 15 mW/cm^2, the fluorescence intensity only decreased, but not quenched, after 2 min of illumination (Figure 6 and Figure S31), demonstrating good photostability of AIE polymersomes. Further, the fluorescence will be greatly decreased after 60 min illumination due to the cyclization[21] of the TPE moiety (Figure S31-S32).

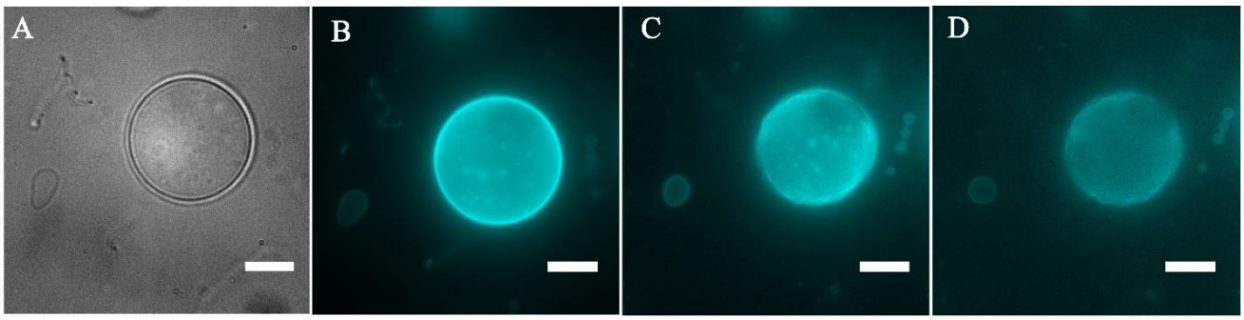

Figure 6. Epifluorescence optical microscopic images of giant vesicles of PEG550-TPE-Chol (*trans/cis* = 60/40). (A) White field. (B-D) Fluorescence images under continuous UV illumination at t = 0 (B), t = 40 sec (C) and t = 60 sec (D). The exposure time of each picture was 300 μsec. Scale bar = 10 μm. LED-UV (365 nm) was used for illumination. The focused intensity on the sample was 15 mW/cm^2.

CONCLUSIONS

Stereoisomer-directed self-assemblies have been demonstrated in this work: *trans*-PEG550-TPE-Chol formed normal vesicles, *cis*-PEG550-TPE-Chol formed cylindrical micelles, and PEG550-TPE-Chol synthesized without isomers' separation (*trans/cis* = 60/40) formed perforated vesicles and membranes with the pores size of 9 - 27 nm. Similar nano-porous vesicles were also obtained by self-assembling the intentionally prepared mixture of *trans*- and *cis*-PEG550-TPE-Chol in the ratio of *trans/cis* = 60/40. All these self-assemblies exhibited high colloidal stability at room temperature for several months without morphological changes.

Under UV illumination of normal intensity for observation and imaging (typically < 0.5 mW/cm^2), these self-assemblies showed AIE fluorescence. Under stronger UV intensity (15 mW/cm^2) and longer illumination time (2 – 30 min), photo-responsive features were recorded due to *trans*-to-*cis* and *cis*-to-*trans* photo-isomerization. Smooth vesicles of *trans*-PEG550-TPE-Chol were perforated by the *cis*-isomers stemmed from the photoisomerization, while cylindrical micelles of *cis*-PEG550-TPE-Chol interweaved to form meshes and perforated membranes. Nano-porous vesicles of PEG550-TPE-Chol upon strong UV light exposure did not show significant change in nanoscale, but in micrometer scale membrane fluctuation was observed by epifluorescence microscopy.

The vesicles of *trans*-PEG550-TPE-Chol can be considered as light-gated polymersomes, where pores of 9-27 nm were generated under strong UV illumination (15 mW/cm^2). They can be traced by their fluorescence under weak UV light and become permeable for small molecules (< 30 nm) under stronger UV light. Nano-porous polymersomes and polymer membranes formed by *trans*- and *cis*- PEG550-TPE-Chol mixture may be promising for applications that require nano-pores as channels for material transportation.

EXPERIMENTAL SECTION

Materials

4-Methoxybenzophenone (≥98%), Titanium tetrachloride ($TiCl_4$, >98%), Boron tribromide (BBr_3, >98%), 4-dimethylaminopyridine (DMAP, >99%), Zn Powder (2.5 cm, >99%), 1-(3-Dimethylaminopropyl)-3-ethylcarbodiimide hydrochloride (EDCI, >98%), Lithium hydroxide (LiOH, ≥98%), Cholesterol (Chol, >95%), Poly (ethylene glycol) methyl ether (MeO-PEG$_n$-OH, n = 12, M_n = 550 Da, M_w/M_n = 1.01) were purchased from Alfa Aesar. Tetramethylrhodamine isothiocyanate–Dextran (TRITC-Dextran, MW = 4400) were purchased from Sigma-Aldrich.

Instruments and characterizations

^{1}H NMR and ^{13}C NMR spectra were recorded on Bruker AV 400 and Bruker AV 500 spectrometers. Chemical shifts δ are given in ppm and referenced to tetramethylsilane (TMS) in $CDCl_3$ (0 ppm). UV spectra were measured on a Milton Ray Spectronic 3000 Array spectrophotometer. Photoluminescence (PL) spectra were recorded on a Horiba FluoroMax Spectrofluorometers. Hydrodynamic diameters of self-assemblies and their distributions in pure water were measured at 25 °C by dynamic light scattering (DLS, Malvern zetasizer 3000HS, UK) with a 633 nm laser. A 90° scattering angle was used for all measurements. Self-assembled morphologies were observed by cryo-electron microscopy (cryo-EM). Cryo-EM images were acquired on a JEOL 2200FS energy-filtered (20 eV slit) field emission gun electron microscope operating at 200 kV using a Gatan US1000 camera. For the sample preparation, a total of 5 μL of samples were deposited onto a 200-mesh holey copper grid (Ted Pella Inc., U.S.A.) and flash-frozen in liquid ethane cooled down at liquid nitrogen temperature using a Leica EM-CPC system. Giant polymersomes were observed by epifluorescence microscopy using a Leica DMR upright microscope equipped with a Retiga Ex*i* CCD camera (Teledyne Technologies) and LED Lamp (λ=365 nm). Images were acquired with Image-Pro Plus (Media Cybernetics) and processed/analyzed using ImageJ. Samples (10 μL) were deposited between a glass slide and cover slip with spacers. The observations were performed with a 100x objective lens (N.A. 1.3). LED lamp (M365L2, λ=365 nm) was used for photoisomerization. The UV intensity was adjusted by a LED Driver LEDD1B. The UV intensity (365 nm) were measured with International Light ILT 1400-A Radiometer/Photometer equipped with SEL005 UV-Visible GaAsP detector.

Synthesis

TPE-2OMe and TPE-2OH in Scheme S1 were synthesized as previously reported (see SI).[36]

Synthesis of TPE-2COOMe. The crude product TPE-2OH (2.18 g, 6.0 mmol) was dissolved in 50 mL of CH_3CN. K_2CO_3 (2.50 g, 18.0 mmol) and methyl 6-bromohexanoate (2.75, 13.2 mol) were added, and the mixture was refluxed for 4h before cooling and filtering. The filtrate was concentrated and purified by flash chromatography to obtain random TPE-2COOMe product (without stereoisomers separation) 1 g (81% yield). If careful chromatography on a silica gel column with an eluent of PE and EA (10:1 *v/v*) was performed, *trans*-TPE-2COOMe and *cis*-TPE-2COOMe were separated. The *trans*-TPE-2COOMe was obtained as white solid and *cis*-TPE-2COOMe as pale-yellow liquid. *Trans*-TPE-2COOMe: ^{1}H NMR ($CDCl_3$, 400 MHz): δ = 7.10- 7.03 (m,10H, Ar*H*), 6.89 (d, *J* = 8.0 Hz, 4H, Ar*H*), 6.59 (d, *J* = 8.1 Hz, 4H, Ar*H*), 3.87 (t, 4H, *J*= 6.2 Hz , ArO$CH_2$$CH_2$), 3.67 (s, 6H,O$CH_3$), 2.34 (t, *J*= 7.3 Hz, 4H, $CH_2$$COOCH_3$), 1.77-1.65 (m, 8H, $CH_2$$CH_2$$CH_2$), 1.50- 1.47 (m, 4H, $CH_2$$CH_2$$CH_2$). ^{13}C NMR ($CDCl_3$, 100 MHz): δ = 174.2, 157.5, 144.5, 139.8, 136.4, 132.7, 131.5, 127.8, 126.3, 113.6, 67.5, 51,7, 34.1, 29.1, 25.8, 24.9. HRMS (ESI) calcd. for ([M+Na] $^+$): $C_{40}H_{44}O_6Na$ 643.30301; Found: 643.30295. *Cis*-TPE-2COOMe: ^{1}H NMR ($CDCl_3$, 400 MHz): δ = 7.06- 7.02 (m,10H, Ar*H*), 6.93 (d, *J* = 7.8 Hz, 4H, Ar*H*), 6.63 (d, *J* = 7.8 Hz, 4H, Ar*H*), 3.89 (t, 4H, *J*= 6.1 Hz, ArO$CH_2$$CH_2$), 3.67 (s, 6H, O$CH_3$), 2.35 (t, *J*= 7.3 Hz, 4H, $CH_2$$COOCH_3$), 1.78- 1.68 (m, 8H, $CH_2$$CH_2$$CH_2$), 1.50- 1.47 (m, 4H, $CH_2$$CH_2$$CH_2$). ^{13}C NMR ($CDCl_3$, 100 MHz): δ = 174.2, 157.5, 144.4, 139.7, 136.4, 132.6, 131.6, 127.7, 126.3, 113.7, 67.5, 51,6, 34.1, 29.1, 25.8, 24.9.

Synthesis of TPE-2COOH. TPE-2COOMe (or its *trans*- or *cis*-isomer) (1.52 g, 2.5 mmol) was dissolved in 80mL of THF/H_2O (*v/v* = 7:1). LiOH (0.31 g, 12.5 mmol) was then slowly added, and the mixture was stirred overnight. THF was removed under reduced pressure and CH_2Cl_2 100 mL added. The pH of the mixture was then adjusted to 1.0 with 1 M HCl before extracting 3

times with DCM. The organic phase was dried over anhydrous $MgSO_4$ and then concentrated to give compound TPE-2COOH (1.32 g, 91% yield) with flash chromatography. *Trans*-TPE-2COOH: ^{1}H NMR ($CDCl_3$, 400 MHz): δ= 7.12- 7.03 (m,10H, Ar*H*), 6.89 (d, *J* = 8.5 Hz, 4H, Ar*H*), 6.59 (d, *J* = 8.4 Hz, 4H, Ar*H*), 3.87 (t, 4H, *J*= 6.3 Hz, ArO*CH*$_2$$CH_2$), 2.38 (t, *J*= 7.4 Hz, 4H, C*H*$_2$COOH), 1.79- 1.66 (m, 8H, CH_2C*H*$_2$$CH_2$), 1.54- 1.46 (m, 4H, CH_2C*H*$_2$$CH_2$). ^{13}C NMR ($CDCl_3$, 100 MHz): δ= 179.3, 157.5, 144.5, 139.8, 136.4, 132.7, 131.5, 127.8, 126.3, 113.7, 67.5, 34.0, 29.1, 25.8, 24.6. HRMS (ESI) calcd. for ([M-H]$^-$): $C_{38}H_{39}O_6$ 591.27521; Found: 591.27569. *Cis*-TPE-2COOH: ^{1}H NMR ($CDCl_3$, 400 MHz): δ= 7.08- 7.01 (m,10H, Ar*H*), 6.91 (d, *J* = 8.1 Hz, 4H, Ar*H*), 6.64 (d, *J* = 8.3 Hz, 4H, Ar*H*), 3.89 (t, 4H, *J*= 6.1 Hz, ArO*CH*$_2$$CH_2$), 2.40 (t, *J*= 7.1 Hz, 4H, C*H*$_2$COOH), 1.80- 1.69 (m, 8H, -C*H*$_2$C*H*$_2$$CH_2$), 1.54- 1.50 (m, 4H, CH_2C*H*$_2$$CH_2$). ^{13}C NMR ($CDCl_3$, 100 MHz): δ= 180.3, 157.6, 144.3, 139.9, 136.5, 132.6, 131.6, 127.7, 126.3, 113.8, 67.6, 34.1, 29.0, 25.7, 24.6.

Synthesis of TPE-Chol-COOH. TPE-2COOH (or its *trans*- or *cis*-isomer) (2.50 g, 4.2 mmol), cholesterol (1.63 g, 4.2 mmol), EDCI (0.89 g, 4.6 mmol), DMAP (0.52 g, 4.2 mmol) and dried CH_2Cl_2 (100 mL) were introduced into a two-necked flask. The mixture was stirred overnight at room temperature. The organic layer was washed with saturated brine solution three times. The combined organic phase was dried over anhydrous Na_2SO_4. The filtrate was concentrated and purified on a silica gel column with an eluent of petroleum ether and ethyl acetate (10:1, *v/v*) to give white solid compound TPE-Chol-COOH (2.21 g, 54 % yield). *Trans*-TPE-Chol-COOH: ^{1}H NMR ($CDCl_3$, 400 MHz): δ= 7.11- 7.00 (m,10H, Ar*H*), 6.89 (d, *J* = 8.0 Hz, 4H, Ar*H*), 6.59 (d, *J* = 8.0 Hz, 4H, Ar*H*), 5.37 (d, *J* = 4.0 Hz, 1H, C=C*H*), 4.65–4.57 (m, 4H, OC*H*), 2.40-2.30 (m, 6H, C*H*$_2$), 2.02-0.85 (m, 51H, C*H*, CH_2, CH_3), 0.68 (s, 3H, CH_3). ^{13}C NMR ($CDCl_3$, 100 MHz): δ=178.6, 173.1, 157.4, 157.4, 144.3, 139.7, 139.6, 139.6, 136.3, 136.3, 132.5, 131.4, 127.6,

126.1, 122.6, 113.5, 77.3, 73.8, 67.4, 67.4, 56.7, 56.1, 50.0, 42.3, 39.8, 39.5, 38.2, 37.0, 36.6, 36.2, 35.8, 34.9, 33.7, 31.9, 31.9, 29.0, 28.3, 28.0, 27.8, 25.6, 24.8, 24.5, 24.3, 23.8, 22.8, 22.6, 21.0, 19.4, 18.7, 11.9. HRMS (ESI) calcd. for ([M-H]$^-$): $C_{65}H_{83}O_6$ 959.61951; Found: 959.62004. *Cis*-TPE-Chol-COOH: ^{1}H NMR ($CDCl_3$, 400 MHz): δ= 7.09- 7.00 (m,10H, ArH), 6.93 (d, J = 8.0 Hz, 4H, ArH), 6.63 (d, J = 8.4 Hz, 4H, ArH), 5.38 (d, J = 4.0 Hz, 1H, C=CH), 4.67–4.59 (m, 4H, OCH), 3.87 (t, 4H, *J*= 6.3 Hz, ArO*CH*$_2$CH$_2$), 2.41-2.30 (m, 6H, C*H*$_2$), 2.05-0.87 (m, 51H, C*H*, C*H*$_2$, C*H*$_3$), 0.69 (s, 3H, CH_3). ^{13}C NMR ($CDCl_3$, 100 MHz): δ= 179.1, 173.2, 157.4, 144.3, 139.7, 139.7, 139.6, 136.4, 136.3, 132.5, 131.4, 127.5, 126.1, 122.7, 113.6, 73.9, 67.4, 67.4, 56.7, 56.2, 50.0, 42.3, 39.8, 39.5, 38.2, 37.0, 36.6, 36.2, 35.8, 34.6, 33.9, 31.9, 31.9, 29.0, 28.3, 28.0, 27.8, 25.7, 24.8, 24.5, 24.3, 23.9, 22.9, 22.6, 21.1, 19.4, 18.8, 11.8.

Synthesis of PEG-TPE-Chol. TPE-Chol-COOH (or its *trans*- or *cis*-isomer) (0.28 g, 0.30 mmol), mPEG-OH (M_n = 550 Da, 0.13 g, 0.23 mmol), EDCI (62.2 mg, 0.33 mmol), DMAP (39.7 mg, 0.33 mmol) and dried CH_2Cl_2 (50 mL) were introduced into two-necked flask. The mixture was stirred overnight at room temperature. The organic layer was washed with saturated brine solution 3 times. The combined organic phase was dried over anhydrous Na_2SO_4. The filtrate was concentrated and purified on a silica gel column with an eluent of dichloromethane and methanol (35:1, *v/v*) to give product PEG550-TPE-Chol (or *trans*-PEG550-TPE-Chol or *cis*-PEG550-TPE-Chol). ^{1}H NMR spectra of PEG550-TPE-Chol, *trans*-PEG550-TPE-Chol and *cis*-PEG550-TPE-Chol are shown in Figure S3, S13-15 below.

ASSOCIATED CONTENT

Supplementary information. ^{1}H NMR and ^{13}C NMR spectra of all compounds. SEC spectra of the synthesized *trans*- and *cis*- PEG550-TPE-Chol. The crystal data and structure of *trans*-TPE-

2COOMe. Supplemental data of photoluminescence spectra. Supplemental data of DLS. Supplemental cryo-EM images of the assemblies.

Supplementary Movie. Movie of giant polymersomes under continuous UV illumination recorded with epifluorescence optical microscope.

Preprint Version. Hui Chen, Yujiao Fan, Xia Yu, Vincent Semetey, Sylvain Trépout, and Min-Hui Li. Light-Gated Nano-Porous Polymersomes from Stereoisomer-Directed Self-Assemblies. 2020, DOI: 10.21203/rs.3.rs-36308/v1. Research Square. https://www.researchsquare.com/article/rs-36308/v1 (June 24, 2020).

AUTHOR INFORMATION

Corresponding Author

* Min-Hui LI

Email: min-hui.li@chimieparistech.psl.eu

Author contributions: The manuscript was written through contributions of all authors. H.C. and M.-H.L. designed research; H.C., Y.F., Y.X. and M.-H.L. performed research; H.C. and S.T contributed to the cryo-EM imaging and analyses; Y.F. and V.S. contributed to the observation by fluorescent microscopy. H.C. and M.-H.L. analyzed data and wrote the paper.

Competing and financial interests: The authors declare no competing financial interests.

ACKNOWLEDGMENT

This work was financially supported by the French National Research Agency (ANR-16-CE29-0028). Y. Fan gratefully acknowledges the China Scholarship Council for funding her PhD scholarship. We thank B. Z. Tang from Hong Kong University of Science & Technology and X. Xing from Shanghai Jiao Tong University for fruitful discussions, and P. Keller from

Institut Curie for critical reading of the manuscript. The PICT-IBiSA of Institut Curie is acknowledged for providing access to cryo-EM facility in Orsay.

REFERENCES

(1). Angelescu, D. G.; Linse, P. Viruses as Supramolecular Self-Assemblies: Modelling of Capsid Formation and Genome Packaging. *Soft Matter* **2008,** *4*, 1981−1990.

(2). Myschik, J.; Lendemans, D. G.; McBurney, W. T.; Demana, P. H.; Hook, S.; Rades, T. On the Preparation, Microscopic Investigation and Application of ISCOMs. *Micron* **2006,** *37*, 724−734.

(3). Edwards, K.; Gustafsson, J.; Almgren, M.; Karlsson, G. Solubilization of Lecithin Vesicles by a Cationic Surfactant: Intermediate Structures in the Vesicle-Micelle Transition Observed by Cryo-Transmission Electron Microscopy. *J. Colloid Interface Sci.* **1993,** *161*, 299−309.

(4). Almgren, M. Stomatosomes: Perforated Bilayer Structures. *Soft Matter* **2010,** *6*, 1383−1390.

(5). Ljusberg-Wahren, H.; Gunnarsson, T.; Wannerberger, L.; Gustafsson, J.; Almgren, M.; Krog, N. Micelles and Liquid Crystals in Aqueous Diglycerol Monodecanoate Systems. In *The Colloid Science of Lipids*; Lindman, B., Ninham, B. W., Eds.; Steinkopff, 1998; pp 99−104.

(6). Van Dam, L.; Karlsson, G.; Edwards, K. Direct Observation and Characterization of DMPC/DHPC Aggregates under Conditions Relevant for Biological Solution NMR. *BBA-Biomembranes* **2004,** *1664*, 241−256.

(7). Kim, J. K.; Lee, E.; Lim, Y. b.; Lee, M. Supramolecular Capsules with Gated Pores from an Amphiphilic Rod Assembly. *Angew. Chem. Int. Ed.* **2008,** *47*, 4662−4666.

(8). Berlepsch, H. v.; Thota, B.; Wyszogrodzka, M.; de Carlo, S.; Haag, R.; Böttcher, C. Controlled Self-Assembly of Stomatosomes by Use of Single-Component Fluorinated Dendritic Amphiphiles. *Soft matter* **2018,** *14*, 5256−5269.

(9). Alessandri, K.; Feyeux, M.; Gurchenkov, B.; Delgado, C.; Trushko, A.; Krause, K.-H.; Vignjević, D.; Nassoy, P.; Roux, A. A 3D Printed Microfluidic Device for Production of Functionalized Hydrogel Microcapsules for Culture and Differentiation of Human Neuronal Stem Cells (HNSC). *Lab Chip* **2016,** *16*, 1593−1604.

(10). Alessandri, K.; Sarangi, B. R.; Gurchenkov, V. V.; Sinha, B.; Kießling, T. R.; Fetler, L.; Rico, F.; Scheuring, S.; Lamaze, C.; Simon, A. Cellular Capsules as a Tool for Multicellular Spheroid Production and for Investigating the Mechanics of Tumor Progression *in Vitro*. *PNAS* **2013,** *110*, 14843−14848.

(11). Piñol, R.; Jia, L.; Gubellini, F.; Lévy, D.; Albouy, P.-A.; Keller, P.; Cao, A.; Li, M.-H. Self-Assembly of PEG-B-Liquid Crystal Polymer: The Role of Smectic Order in the Formation of Nanofibers. *Macromolecules* **2007,** *40*, 5625−5627.

(12). Zhou, Y.; Briand, V. A.; Sharma, N.; Ahn, S.-k.; Kasi, R. M. Polymers Comprising Cholesterol: Synthesis, Self-Assembly, and Applications. *Materials* **2009,** *2*, 636−660.

(13). Xie, Y.; Li, Z. Recent Advances in the Z/E Isomers of Tetraphenylethene Derivatives: Stereoselective Synthesis, AIE Mechanism, Photophysical Properties, and Application as Chemical Probes. *Chem. Asian J.* **2019,** *14*, 2524−2541.

(14). Peng, H.-Q.; Zheng, X.; Han, T.; Kwok, R. T.; Lam, J. W.; Huang, X.; Tang, B. Z. Dramatic Differences in Aggregation-Induced Emission and Supramolecular Polymerizability of Tetraphenylethene-Based Stereoisomers. *J. Am. Chem. Soc.* **2017,** *139*, 10150−10156.

(15). Peng, H. Q.; Liu, B.; Wei, P.; Zhang, P.; Zhang, H.; Zhang, J.; Li, K.; Li, Y.; Cheng, Y.; Lam, J. W. Y.; Zhang, W.; Lee, C. S.; Tang, B. Z. Visualizing the Initial Step of Self-Assembly and the Phase Transition by Stereogenic Amphiphiles with Aggregation-Induced Emission. *ACS Nano* **2019,** *13*, 839−846.

(16). Bunker, C. E.; Hamilton, N. B.; Sun, Y. P. Quantitative Application of Principal Component Analysis and Self-Modeling Spectral Resolution to Product Analysis of Tetraphenylethylene Photochemical Reactions. *Anal. Chem.* **1993,** *65*, 3460−3465.

(17). Mei, J.; Hong, Y.; Lam, J. W.; Qin, A.; Tang, Y.; Tang, B. Z. Aggregation‐Induced Emission: The Whole Is More Brilliant Than the Parts. *Adv. Mater.* **2014,** *26*, 5429−5479.

(18). Mei, J.; Leung, N. L.; Kwok, R. T.; Lam, J. W.; Tang, B. Z. Aggregation-Induced Emission: Together We Shine, United We Soar! *Chem. Rev.* **2015,** *115*, 11718−11940.

(19). Li, J.; Wang, J.; Li, H.; Song, N.; Wang, D.; Tang, B. Z. Supramolecular Materials Based on AIE Luminogens (AIEgens): Construction and Applications. *Chem. Soc. Rev.* **2020,** *49*, 1144−1172.

(20). Yan, L.; Zhang, Y.; Xu, B.; Tian, W. Fluorescent Nanoparticles Based on AIE Fluorogens for Bioimaging. *Nanoscale* **2016,** *8*, 2471−2487.

(21). Feng, G.; Liu, B. Aggregation-Induced Emission (AIE) Dots: Emerging Theranostic Nanolights. *Acc. Chem. Res.* **2018,** *51*, 1404−1414.

(22). Mabrouk, E.; Cuvelier, D.; Brochard-Wyart, F.; Nassoy, P.; Li, M.-H. Bursting of Sensitive Polymersomes Induced by Curling. *PNAS* **2009,** *106*, 7294−7298.

(23). Del Barrio, J.; Oriol, L.; Sánchez, C.; Serrano, J. L.; Di Cicco, A.; Keller, P.; Li, M.-H. Self-Assembly of Linear−Dendritic Diblock Copolymers: From Nanofibers to Polymersomes. *J. Am. Chem. Soc.* **2010,** *132*, 3762−3769.

(24). Cui, Z.-K.; Phoeung, T.; Rousseau, P.-A.; Rydzek, G.; Zhang, Q.; Bazuin, C. G.; Lafleur, M. Nonphospholipid Fluid Liposomes with Switchable Photocontrolled Release. *Langmuir* **2014,** *30*, 10818−10825.

(25). Liu, D.; Wang, S.; Xu, S.; Liu, H. Photocontrollable Intermittent Release of Doxorubicin Hydrochloride from Liposomes Embedded by Azobenzene-Contained Glycolipid. *Langmuir* **2017,** *33*, 1004−1012.

(26). Li, L.; Cui, S.; Hu, A.; Zhang, W.; Li, Y.; Zhou, N.; Zhang, Z.; Zhu, X. Smart Azobenzene-Containing Tubular Polymersomes: Fabrication and Multiple Morphological Tuning. *Chem. Commun.* **2020,** *56*, 6237−6240.

(27). Geng, Y.; Dalhaimer, P.; Cai, S.; Tsai, R.; Tewari, M.; Minko, T.; Discher, D. E. Shape Effects of Filaments *Versus* Spherical Particles in Flow and Drug Delivery. *Nat. Nanotechnol.* **2007,** *2*, 249−255.

(28). Zhu, L.; Wang, R.; Tan, L.; Liang, X.; Zhong, C.; Wu, F. Aggregation‐Induced Emission and Aggregation‐Promoted Photo‐Oxidation in Thiophene‐Substituted Tetraphenylethylene Derivative. *Chem. Asian J.* **2016,** *11*, 2932−2937.

(29). Jain, S.; Bates, F. S. On the Origins of Morphological Complexity in Block Copolymer Surfactants. *Science* **2003,** *300*, 460−464.

(30). Antonietti, M.; Förster, S. Vesicles and Liposomes: A Self‐Assembly Principle Beyond Lipids. *Adv. Mater.* **2003,** *15*, 1323−1333.

(31). Israelachvili, J. N.; Mitchell, D. J.; Ninham, B. W. Theory of Self-Assembly of Hydrocarbon Amphiphiles into Micelles and Bilayers. *J. Chem. Soc. Faraday Trans.* **1976,** *72*, 1525−1568.

(32). Oh, H.; Ketner, A. M.; Heymann, R.; Kesselman, E.; Danino, D.; Falvey, D. E.; Raghavan, S. R. A Simple Route to Fluids with Photo-Switchable Viscosities Based on a Reversible Transition between Vesicles and Wormlike Micelles. *Soft Matter* **2013,** *9*, 5025−5033.

(33). Echegoyen, L. E.; Portugal, L.; Miller, S. R.; Hernandez, J. C.; Echegoyen, L.; Gokel, G. W. The First Evidence for Aggregation Behavior in a Lipophilic [2.2. 2]-Cryptand and in 18-Membered Ring Steroidal Lariat Ethers. *Tetrahedron Lett.* **1988,** *29*, 4065−4068.

(34). Murata, K.; Aoki, M.; Suzuki, T.; Harada, T.; Kawabata, H.; Komori, T.; Ohseto, F.; Ueda, K.; Shinkai, S. Thermal and Light Control of the Sol-Gel Phase Transition in Cholesterol-Based Organic Gels. Novel Helical Aggregation Modes as Detected by Circular Dichroism and Electron Microscopic Observation. *J. Am. Chem. Soc.* **1994,** *116*, 6664−6676.

(35). Jung, J. H.; Shinkai, S.; Shimizu, T. Nanometer-Level Sol− Gel Transcription of Cholesterol Assemblies into Monodisperse Inner Helical Hollows of the Silica. *Chem. Mater.* **2003,** *15*, 2141−2145.

(36). Fang, X.; Zhang, Y.-M.; Chang, K.; Liu, Z.; Su, X.; Chen, H.; Zhang, S. X.-A.; Liu, Y.; Wu, C. Facile Synthesis, Macroscopic Separation, E/Z Isomerization, and Distinct AIE Properties of Pure Stereoisomers of an Oxetane-Substituted Tetraphenylethene Luminogen. *Chem. Mater.* **2016,** *28*, 6628−6636.